EXPERIMENTAL AND NUMERICAL INVESTIGATIONS OF UNCONSTRAINED MELTING INSIDE A SPHERICAL CONTAINER

S. F. Hosseinizadeh*, F. L. Tan[1], J. M. Khodadadi[2] and A.A Rabienataj Darzi
*Author for correspondence
Department of Mechanical Engineering, Babol Noshirvani University of Technology
Babol, Iran, E-mail: Hosseinizadeh@nit.ac.ir
[1]Nanyang Technological University, School of Mechanical & Aerospace Engineering, 50 Nanyang Avenue,
Singapore 639798
[2]Prof. of Mechanical Engineering, Auburn University, AL 36849, USA

ABSTRACT

This paper presents a numerical and experimental study of unconstrained melting of phase change materials (PCM) inside a spherical container using n-Octadecane. Experimental and numerical studies are performed for three different wall temperatures of 35 °C, 40 °C and 45 °C with an initial sub-cooling of 1 °C. Transient numerical simulations are performed for axi-symmetric melting inside a sphere using the Fluent 6.3 software. The results from experiments data and numerical simulations show that heat conduction through the container's wall initiates melting of the solid PCM. Thereafter, the solid PCM sinks, in turn pushing liquid PCM to the top of sphere. At the top and side of the sphere, natural convection is established due to the replacing of warm liquid PCM with sinking cooler liquid. The results show that the rate of melting at the bottom is higher than the top due to the sinking of solid PCM to the bottom and promoting heat conduction from inner wall of sphere. Experimental results show that the variation of liquid fraction has a nonlinear dependence on time and complete melting of PCM occurs after 80, 90 and 160 minutes for wall temperatures of 35 °C, 40°C and 45 °C, respectively. Numerical simulation results gave earlier complete melting times compared to the experimental results.

INTRODUCTION

Several studies are carried out on phase change materials over the last three decades. Phase change materials are very interesting due to their absorbing of large amount of energy as latent heat at a constant phase transition temperature. These materials can be used for passive heat storage. Major disadvantage of the PCM is related to their low thermal conductivity which impedes high rate of charge and discharge of heat flux. These types of materials have many useful properties including heat source at constant temperature, heat recovery with small temperature drop, high storage density, melting point which matches the application, low vapor pressure (1 bar) at the operational temperature, and chemical stability and non-corrosiveness. These properties allow the PCM to be used in many industrial applications such as thermal storage of solar energy [1-6], thermal management of electronic devices [7-9], thermal storage in buildings [10,11], cooling of engines [12,13].

Following the literature, according to Telkes and Raymond [14], the first study of phase change materials was carried out in the 1940s. There are few work reported until the 1970s. After that, the first study on PCM was presented by Barkmann and Wessling [15] for use in buildings, and later by other researchers [16-18]. Sokolov and Keizman [19] presented applications of PCM in a solar collector for first time at 1991, and later by others, e.g. Rabin et al. [20], Enibe [21, 22], and Tey et al. [23]. Also, there are a few review papers on energy thermal storage and phase change material [24, 25]. Following them, a beneficial review of thermal energy storage based on PCM was presented by Zalba et al. [26]. They classified types of PCM based on material properties, heat transfer and its applications.

In recent years, researchers have shown great interest in using PCM because of greenhouse gas emission and increasing cost of fossil fuels. Majority of their experimental and numerical study are related to saving of energy in building structures and solar collectors. Wang et al. [27] investigated numerically the effect of orientation for PCM based on hybrid heat sinks for electronic devices (plate fin heat sink that immerse in PCM). They found that orientation limited the effect of thermal performance of hybrid cooling system. Stritih [28] investigated an experimental study of heat transfer in a rectangular PCM thermal storage with fins. He selected paraffin as PCM

material. He showed that fin effectiveness during solidification increased up to 3.06 times and then decreased.

Khodadadi and Zhang [29] studied the effect of buoyancy-driven convection on constrained melting of PCM in a spherical container numerically. They used the single–domain enthalpy formulation and the Darcy's law for simulation of phase change phenomenon and porous media treatment. Their results showed the rate of melting in top region of sphere is faster than in bottom region due to increasing of conduction term of heat transfer. They also investigated the effect of the Prandtl number on the flow and melting patterns.

Assis et al. [30] investigated both numerically and experimentally on melting in a spherical shell. They performed their numerical study using the commercial code Fluent 6.0. Computational results had good agreement with experimental results for different wall temperatures and different shell diameters. They presented a correlation for the melting fraction based on the Grashof, Stefan and Fourier numbers. They performed another combined experimental and numerical study on the solidification of PCM inside a spherical shell with various diameters [31].

Tan and Leong [32] carried out an experimental study of solidification of pure n-Octadecane within two rectangular cells with different aspect ratios and three different constant heat fluxes. Their results showed that a faster rate of solidification occurred at higher heat rates and smaller aspect ratios. They carried out another experimental investigation of conjugate solidification inside a thick mold [33]. They used n-Octadecane as PCM that was superheated initially. Their experiments were carried out for subcooled and non-subcooled walls. They found that the solidification fraction is directly proportional to cubic root of time and changes linearly with time for subcooled and non-subcooled wall conditions, respectively.

Khodadadi and Hosseinizadeh [34] performed a numerical study on improvement of thermal storage energy using nanoparticle-enhanced phase change material (NEPCM). They used water and copper nanoparticle as nanofluid that enhance the thermal conductivity of base material. They obtained higher heat release rate using NEPCM instead of PCM.

Tan et al. [35] presented an experimental and computational study of constrained melting of PCM inside a spherical capsule. Their investigations showed that numerical results have some delay compared to experimental finding. They found that this delay could be related to the thermal stratification within the constant temperature bath that enclosed the capsule.

Tan [36] investigated an experimental study of constrained and unconstrained melting in a spherical container using n-Octadecane as PCM that was initially subcooled to 1 °C. He indicated that the solid PCM sinks to the bottom of sphere due to gravity whereas the PCM is restrained from sinking under the constrained condition.

A combined numerical and experimental study of unconstrained melting in a spherical container following the work of [36] is presented in this paper. Results show a noticeable agreement between the numerical and experimental results. Details of the experimental set-up and computational procedures are discussed in following sections.

NOMENCLATURE

C	[kg/m³s]	Mushy zone constant
C_P	[J/kg K]	Specific heat
g	$[m^2 s^{-1}]$	Gravitational acceleration
h	[J/kg]	Sensible enthalpy
H	[J/kg]	Enthalpy
k	[W/mK]	Thermal conductivity
L	[J/kg]	Latent heat of fusion
T	[K]	Temperature
u	[m/s]	velocity
μ	[kg/ms]	Dynamic viscosity of the fluid
ρ	[kg/m³]	Density
V	[m/s²]	Kinematic viscosity
β	-	Liquid fraction

EXPERIMENTAL SET-UP

Paraffin wax n-Octadecane is used as the phase change material in this study. Its properties are reported in Table 1.

Table 1 Properties of n-Octadecane wax paraffin

Solidus/liquidus temperature	27.5°C /28.5°C
Density(solid/liquid)	870 / 772 kg/m³
Kinematics Viscosity	5×10^{-6} m²/s
Specific Heat(solid/liquid)	1990 / 2330 J/kg K
Thermal Conductivity	0.1505 W/m K
Latent Heat of Fusion	241.3 kJ/kg
Thermal Expansion Coefficient	0.00091 K⁻¹

Experimental study was conducted for unconstrained melting of the PCM. Complete details of experimental set-up are described by Tan [36]. The main components of the experimental set-up consisted of a water tank, a spherical container, several type-K thermocouples, refrigerated bath and the HP data acquisition unit as shown in Figure 1. The material of spherical container is Plexiglas. As shown in Figure 2, 11 thermocouples are positioned in the spherical container and the enclosing water tank for measuring the temperature variations during the process. Thermocouples are connected to the HP data acquisition unit to record the temperature variations versus time. At the start of the experiment, the spherical container is set in a water bucket to attain the initial subcooling temperature of 1 °C. Then, it is transferred to the warm water tank. The temperature of water is controlled with a refrigerated bath. The level of water is kept constant by controlling the inlet and outlet valves. This process takes a few minutes to reach a stable temperature around the sphere. It should be mentioned that this time lag must be accounted for when the numerical and experimental results are compared. The numerical results are presented for three outer constant temperatures of 35, 40 and 45°C at a position far enough from the sphere in the water bath. This distance has been selected from the work of Tan [36] by replacing two other thermocouples.
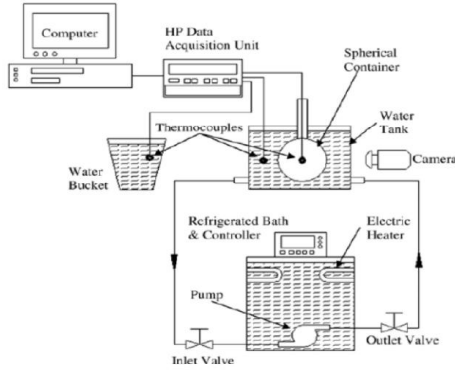
Figure 1 Schematic diagram of experimental set-up

GOVERNING EQUATIONS

In the numerical study, the flow is considered unsteady, laminar, incompressible and two-dimensional. Viscous dissipation term is considered negligible, so that the viscous incompressible flow and the temperature distribution inside the sphere are described by the Navier–Stokes and thermal energy equations, respectively.

Consequently, the continuity, momentum, and thermal energy equations can be expressed as follows:
Continuity:

$$\partial_t(\rho) + \partial_i(\rho u_i) = 0 \tag{1}$$

Momentum:

$$\partial_t(\rho u_i) + \partial_j(\rho u_i u_j) = \mu \partial_{jj} u_i - \partial_i P + \rho g_i + S_i \tag{2}$$

Thermal Energy:

$$\partial_t(\rho h) + \partial_t(\rho \Delta H) + \partial_i(\rho u_i h) = \partial_i(k \partial_i T) \tag{3}$$

In these relations, u_i is the fluid velocity, ρ is the PCM's density, μ is the dynamics viscosity, P is the pressure, g is the gravitational acceleration, k is the thermal conductivity and h is sensible enthalpy that is defined as following [37]:

$$h = h_{ref} + \int_{T_{ref}}^{T} C_p dT \tag{4}$$

The enthalpy, H, is therefore:

$$H = h + \Delta H \tag{5}$$

where ΔH being the latent heat content may vary between zero (solid) and L (liquid), the latent heat of the PCM. Therefore liquid fraction, β, can be defined as following:

$$\beta = \begin{cases} \dfrac{\Delta H}{L} = 0 & \text{if } T < T_{solidus} \\[2mm] \dfrac{\Delta H}{L} = 1 & \text{if } T > T_{liquidus} \\[2mm] \dfrac{\Delta H}{L} = \dfrac{T - T_{solidus}}{T_{liquidus} - T_{solidus}} & \text{if } T_{solidus} < T < T_{liquidus} \end{cases} \tag{6}$$

In equation 2, S_i is the Darcy's law damping terms (as source term) that are added to the momentum equation due to phase change effect on convection. It is defined as:

$$S_i = \frac{C(1 - \beta)^2}{\beta^3} u_i \tag{7}$$

That coefficient C is a mushy zone constant that is fixed to 10^5 kg/m^{3}s for the present study [37].
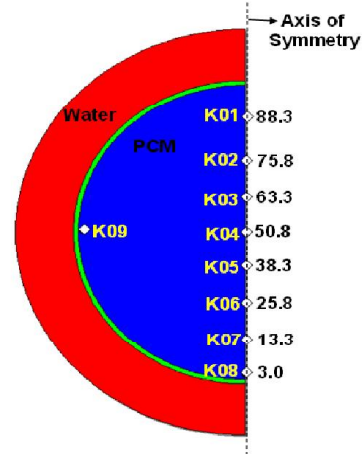

Figure 2 Schematic diagram of computational domain

NUMERICAL PROCEDURE

Numerical study of the present problem is carried out by using the commercial code Fluent 6.3.26. The computational domain of the axi-symmetric model is shown in Figure 2. The sphere's inner radius and wall thickness are 101.66 and 1.5 mm, respectively. The thermal conductivity of Plexiglas is equal to 0.81 (W/m K). In the present simulation, the spherical container was surrounded by another spherical container containing hot water for matching the conditions of the experimental set-up. The temperature of water is assumed to vary linearly from a subcooled temperature to the temperature of container wall (i.e. 27°C to 35°C, 40°C or 45°C). In order to solve the momentum and energy equations, the first order differencing scheme and the SIMPLE method for pressure-velocity coupling are used. Also the PRESTO scheme is adopted for the pressure correction equation. The under-relaxation factors for the velocity components, pressure correction, thermal energy and liquid fraction are 0.3, 0.1, 1 and 0.9, respectively. Different grid densities are selected and tested to ensure independency of solution from the adopted grid density based on comparison of melting fraction and streamline contours. An arrangement of 9,310 grids was found sufficient for present study. Adoption of fine grid distribution in the radial direction allows the use of longer time steps. The time duration to achieve full melting is a good indicator of time step dependence. The PCM melted after 47.4, 58.2 and 60.7 minutes with time step increments of 0.05, 0.02 and 0.01 seconds for wall a temperature of 40°C, respectively. Therefore, the time step is set to 0.02 seconds. The number of iterations for every time step was fixed at 50 that was found sufficient to satisfy convergence criteria (10⁻⁵).

RESULTS AND DISCUSSION

The contours of the PCM at various time instants for the unconstrained melting process are presented in Figure 3. In this figure, results of numerical study (right column) are compared with the experimental observations (left column) for the wall temperature of 40°C. The solid and liquid PCM are opaque white and transparent, respectively for the experimental results, whereas colorized contours of temperature are utilized for presenting the numerical results.
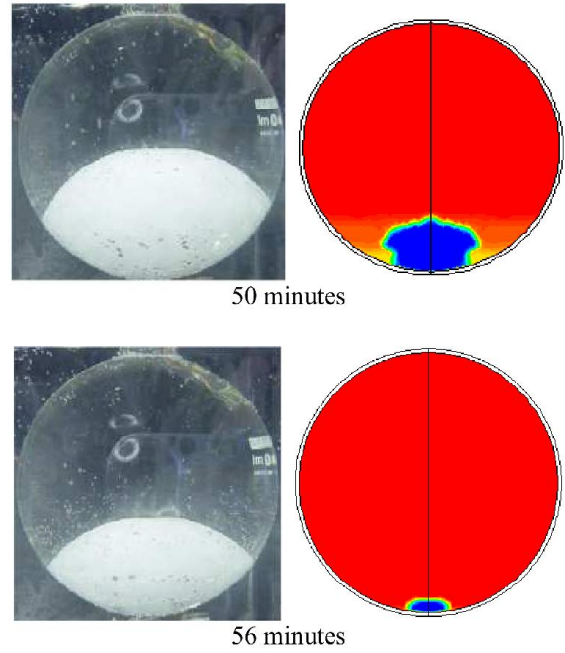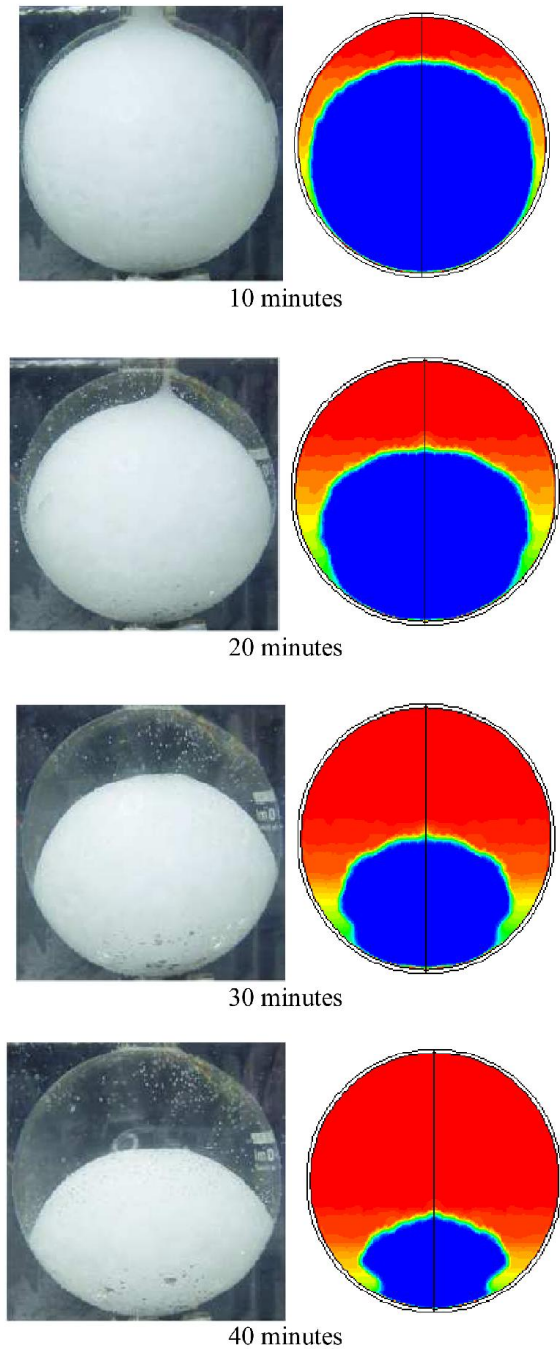

10 minutes

20 minutes

30 minutes

40 minutes

50 minutes

56 minutes

Figure 3 Experimental and computational unconstrained melting at 40°C with an initial subcooling of 1°C

It can be seen that for both approaches, solid PCM sinks to the bottom of sphere due to gravity force since it is heavier in relation to the liquid PCM. Thus, the solid PCM is in contact with the bottom hot surface of sphere at every time. But, this is not a fully contact, while a very thin fluid layer is seen between the inner wall and the solid PCM in every time during the melting. At the start, the outer surface of solid PCM was in contact with the inner wall of sphere so that heat conduction dominates between solid and wall. This causes the formation of a thin layer of liquid between the solid PCM and sphere. As time progresses, the molten zone expanded and the liquid layer grows. The liquid film formed at the bottom of the solid PCM is squeezed down by the sinking heavier solid. The squeezed liquid film is then pushed upward along the inner surface of the sphere, occupying the region above the solid PCM. As the warm liquid rises to the top portion of the sphere, the cooler liquid is replaced and forced to sink toward the solid PCM. Thus, natural convection in combination with a hot rising curved wall jet dominates in the top and side regions of the sphere, while pure heat conduction occurs at the bottom region of sphere between inner wall and the solid PCM. The melting rate at the bottom region of the sphere decreases with time due to the solid PCM becoming smaller and the area of its contact with the bottom surface of sphere shrinking. It should also be mentioned that computed flow field exhibit an unstable and complicated structure near the bottom region of sphere that bring about formation of waviness on the solid-liquid interface. The computed and experimental variations of the liquid fraction against time for three wall temperature are shown in Figure 4. The general trends of both approaches are similar. But it can be observed that numerical results have earlier complete melting time compared to the experimental results. .
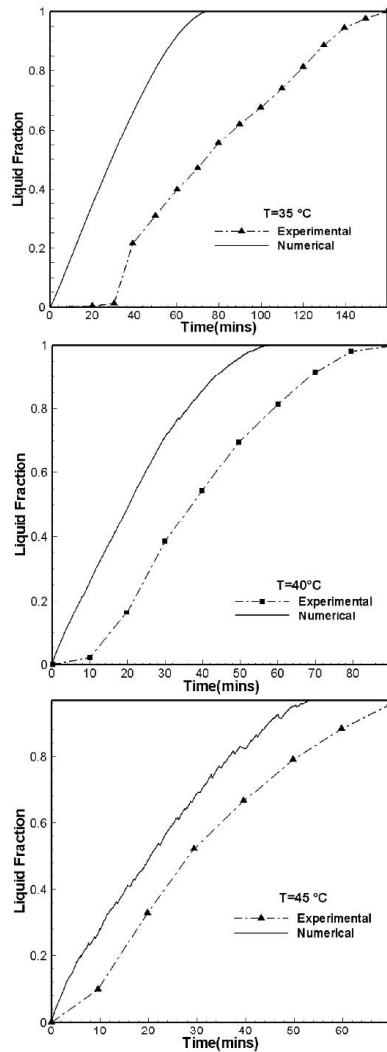
for each point (of thermocouple position) attain the final temperature (that is equal to wall temperature) earlier than experimental result.
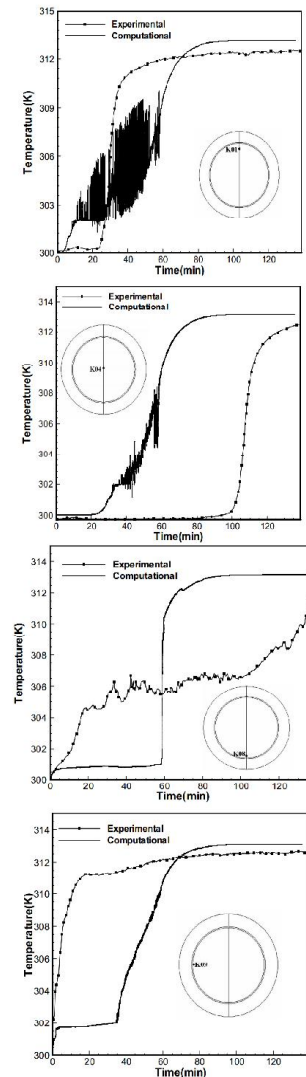

Figure 4 Variations of the liquid fraction versus time for wall temperatures of 35°C, 40°C and 45°C

As can be seen, there is a gap between numerical and experimental results. For this reason, if the numerical results are shifted 15 minutes forward, numerical and experimental findings would agree reasonably well. Experimental results depict that the variation of liquid fraction has nonlinear change with respect to time whereas full melting of PCM occurs at 80, 90 and 160 minutes for wall temperature of 35 °C, 40°C and 45 °C, respectively.

Measured transient temperature readings are compared to the computational predictions for a wall temperature of 40°C in Figure 5. Among the three thermocouples closest to the inner wall of the sphere (K01, K08 and K09), the one that sits on the horizontal plane that contains the center of the sphere (K09) exhibits the fastest rise and the greatest deviation from the initial subcooling temperature. The computed temperature coinciding with the location of the thermocouple at the top of the PCM (K01) register marked unsteadiness early on as the liquid is formed. Similar but less noticeable trends are observed at the center of the sphere. As it is expected, numerical results

Figure 5 Comparison of the computed and measured temperatures at different position for wall temperature of 40°C

CONCLUSIONS
The Following conclusions are drawn based on the present experimental and computational study:
1- Heat conduction dominates at the beginning of melting for all zones of the sphere. After a short time period, the solid PCM sinks and the liquid rises up to top half of sphere. Thus, natural convection is promoted at top half of sphere where melting rate is slower than bottom half.
2- The greatest discrepancy between the numerical and experimental elapsed time for melting is related to starting time of experimental set-up. If this time is eliminated, the results of numerical and experimental are in a better agreement.

REFERENCES

[1] Lane G.A., Solar Heat Storage: Latent Heat Material, vol. II, *Technology, CRC Press*, Florida, 1986.

[2] Kamimoto M., Abe Y., Sawata S., Tani T. and Ozawa T., Latent heat storage unit using form-stable high density polyethylene for solar thermal applications, *Proceedings of the International Symposium on Thermal Application of Solar Energy*, Hakone (Kanagawa, Japan), 1985.

[3] Hadjieva M., Kanev S. and Argirov J., Thermo physical properties of some paraffins applicable to thermal energy storage, *Solar Energy Mater. Solar Cells*, Vol. 27, 1992, pp. 181–187.

[4] Morcos V.H., Investigation of a latent heat thermal energy storage system, *Solar Wind Technology.*, Vol.7, No.2/3, 1990, pp.197–202.

[5] Rabin Y., Bar-Niv I., Korin E. and Mikic B., Integrated solar collector storage system based on a salt-hydrate phase change material, *Solar Energy*, Vol. 55, 1995, pp. 435–444.

[6] S.O. Enibe, Parametric effects on the performance of a passive solar air heater with storage, Proceedings of the World Renewable Energy Congress WII, Cologne (Germany), 2002.

[7] Cabeza L.F., Roca J., Nogues M., Zalba B. and Marin J.M, Transportation and conservation of temperature sensitive materials with phase change materials: state of the art, *IEA ECES IA Annex 17 2nd Workshop*, Ljubljana (Slovenia), 2002.

[8] Cuevas-Diarte M.A., Calvet-Pallas T., Tamarit J.L., Oonk H.A.J., Mondieig D. and Haget Y., Nuevos materials termoajustables, *Mundo Cient_ifico*, June 2000.

[9] Pal D. and Joshi Y., Application of phase change materials for passive thermal control of plastic quad flat packages: a computational study, *Numerical Heat Transfer*, Vol. 30, Part A, 1996, pp. 19–34.

[10] Koschenz M. and B. Lehmann, Development of a thermally activated ceiling panel with PCM for application in lightweight and retrofitted buildings, *Energy and Buildings*, Vol. 36, 2002, pp. 567–578.

[11] Kissock J.K., Hannig J.M., Whitney T.I. and Drake M.L., Testing and simulation of phase change wallboard for thermal storage in buildings, *Proceedings of 1998 International Solar Energy Conference*, New York, USA, 1998, pp. 45–52.

[12] Bellettre J., Sartre V., Biais F. and Lallemand A., Transient state study of electric motor heating and phase change solid–liquid cooling, Applied Thermal Engineering, Vol. 17, No.1, 1997, pp. 17–31.

[13] Vasiliev L.L., Burak V.S., Kulakov A.G., Mishkinis D.A. and Bohan, P.V. Latent heat storage modules for preheating internal combustion engines: application to a bus petrol engine, *Applied Thermal Engineering*, Vol. 20, 2000, pp. 913–923.

[14] Telkes M., Thermal storage for solar heating and cooling, *Proceedings of the Workshop on Solar Energy Storage Subsystems for the Heating and Cooling of Buildings*, Charlottesville (Virginia, USA), 1975.

[15] Barkmann H.G. and Wessling F.C., Use of buildings structural components for thermal storage, *Proceedings of the Workshop on Solar Energy Storage Subsystems for the Heating and Cooling of Buildings*, Charlottesville (Virginia, USA), 1975.

[16] Hawes D.W., Feldman D. and D. Banu, Latent heat storage in building materials, *Energy Buildings*, Vol. 20, 1993, pp. 77–86.

[17] Morikama Y., Suzuki H., Okagawa F. and Kanki K., A development of building elements using PCM, *Proceedings of the International Symposium on Thermal Application of Solar Energy*, Hakone (Kanagawa, Japan), 1985.

[18] Lee C.H. and Choi H.K., Crystalline Morphology in High-Density Polyethylene/Paraffin Blend for Thermal Energy Storage, *Polymer Composites*, Vol. 19, No. 6, 1998, pp. 704–708.

[19] Sokolov M. and Keizman Y., Performance indicators for solar pipes with phase change storage, *Solar Energy*, Vol. 47, 1991, pp. 339–346.

[20] Rabin Y., Bar-Niv I., Korin E. and Mikic B., Integrated solar collector storage system based on a salt-hydrate phase change material, *Solar Energy*, Vol. 55, 1995, pp. 435–444.

[21] S.O. Enibe, Performance of a natural circulation air heating system with phase change material energy storage, *Renewable Energy*, Vol. 27, 2002, pp. 69–86.

[22] Enibe S.O., Parametric effects on the performance of a passive solar air heater with storage, *Proceedings of the World Renewable Energy Congress WII*, Cologne (Germany), 2002.

[23] Tey J., Fernandez R., Rosell J., Ibanez M., Solar collector with integrated storage and transparent insulation cover, *Proceedings of Eurosun*, Bologna (Italy), 2002.

[24] Agyenim F., Hewitt N., Eames P., Smyth M., A review of materials, heat transfer and phase change problem formulation for latent heat thermal energy storage systems (LHTESS),*Renewable and Sustainable Energy Reviews*, Vol. 14, 2010, pp. 615–628.

[25] Farid M.M., Khudhair A.M., Razack S.A.K., Al-Hallaj S., A review on phase change energy storage: materials and applications, *Energy Conversion and Management*, Vol. 45 , 2004, pp.1597–1615.

[26] Zalba b., Marin J.M., Cabeza L.F., Mehling H., Review on thermal energy storage with phase change: materials, heat transfer analysis and applications, *Applied Thermal Engineering*, Vol. 23, 2003, pp. 251–283.

[27] Wang X.Q., Mujumdar A.S. and Yap C., Effect of orientation for phase change material (PCM)-based heat sinks for transient thermal management of electric components, *International Communications in Heat and Mass Transfer*, Vol. 34, 2007, pp. 801–808

[28] Stritih U., An experimental study of enhanced heat transfer in rectangular PCM thermal storage, *International Journal of Heat and Mass Transfer*, Vol. 47, 2004, pp. 2841–2847.

[29] Khodadadi J.M. and Zhang Y., Effects of buoyancy-driven convection on melting within spherical containers, International Journal of Heat and Mass Transfer, Vol. 44, 2001, pp. 1605-1618.

[30] Assis E., Katsman L., Ziskind G. and Letan R., Numerical and experimental study of melting in a spherical shell, *International Journal of Heat and Mass Transfer*, Vol. 50, 2007, pp. 1790–1804.

[31]] Assis E., Ziskind G. and Letan R., Numerical and Experimental Study of Solidification in a Spherical Shell, *Journal of heat transfer*, Vol. 31,2009,****

[32] Tan F.L. and Leong K.C., an experimental investigation of solidification in a rectangular enclosure under constant heat rate conditions, *International Communication in Heat and Mass Transfer*, Vol. 26, No. 7, 1999, pp. 925-934.

[33] Tan F.L. and Leong K.C., Conjugate solidification inside a thick mold, *Journal of Materials Processing Technology*, Vol. 89–90, 1999, pp.159–164

[34] Khodadadi J.M. and Hosseinizadeh S.F., Nanoparticle-enhanced phase change materials (NEPCM) with great potential for improved thermal energy storage, *International Communications in Heat and Mass Transfer*, Vol. 34, 2007, pp. 534–543.

[35] Tan F.L., Hosseinizadeh S.F., Khodadadi J.M. and Fan L., Experimental and computational study of constrained melting of phase change materials (PCM) inside a spherical capsule, *International Journal of Heat and Mass Transfer*, Vol. 52, 2009, pp. 3464–3472.

[36] Tan F.L., Constrained and unconstrained melting inside a sphere, *International Communications in Heat and Mass Transfer*, Vol. 35, 2008, pp. 466–475.

[37] www.FLUENT.com